METHODS FOR IMPROVING SEISMIC EVENT LOCATION PROCESSING

Clifford H. Thurber, Haijiang Zhang, Charlotte A. Rowe, and William J. Lutter

University of Wisconsin-Madison

Sponsored by Defense Threat Reduction Agency

Contract No. DTRA01-01-C-0085

ABSTRACT

Our research program consists of four components, each involving some aspect of multiple-event analysis: (1) high-precision waveform cross-correlation (WCC) for arrival time estimation, (2) robust event clustering, (3) waveform decomposition and source wavelet deconvolution reshaping, (4) double-difference (DD) multiple-event location and tomography. Our research is focusing initially on the development and testing of these seismic analysis methods using "ground-truth" datasets at different scales (local and regional), and will be followed by the application of these methods to "test-bed" seismic datasets, including tests on real-time data streams.

We are constructing two regional ground-truth datasets, one for New Mexico and one for California. The former dataset is from the New Mexico Tech short-period network and is dominated by small explosions, whereas the latter is from the UC-Berkeley broadband network and contains relatively large earthquakes (about 260 events of magnitude 4.3 and above). In each case, the ground-truth dataset will be used initially for algorithm assessment purposes and later as a "reference event" dataset for clustering and locating new events. The New Mexico "training" dataset is undergoing final grooming. For the California dataset, we have affirmed the quality of the ground-truth location information by carrying out a DD location analysis using catalog time-difference data. We also present initial results of hierarchical cross-correlation analysis applied to the California dataset.

We have completed the modifications to the integer portion of the cross-correlation software, adding the multiple eigentaper approach to provide improved integer correlation statistics. The modifications to the program logic provide the initial step for subsequent adaptation towards multiple frequency-scale correlations. In addition, modifications have been completed to interface the WCC software with our new DD tomography code (discussed below). We are preparing the California dataset for further DD location analysis and for processing with the regional-scale tomography code under development. At the same time, we will experiment with clustering and waveform decomposition and reshaping techniques to expand the ability to use WCC on large datasets. Efforts have also begun on an Earthworm-MatSeis real-time interface, including the generation of CSS database files from Earthworm.

We have developed a new DD tomography method that uses high-precision WCC relative arrival time picks as well as differential and absolute catalog arrival-time picks. "Double-difference" refers to the residual between the observed differential arrival-time picks and the predicted differential arrival-times. If two sources have almost identical source mechanisms and the differential signal scattering due to velocity heterogeneity along the ray path is minor, they will produce similar waveforms at the same station, allowing for the use of WCC to determine precise differential times. Compared to absolute travel-time picks, relative arrival-time picks obtained using WCC methods have a precision to the sub-sample level. When two sources are far away from each other so that their waveforms are not similar, we just use the relative catalog arrival-time pick differences. We also use the absolute travel-time picks to constrain the absolute event locations.

Our new DD tomography method has been applied to the Hayward fault, California, as an initial test to compare to previously published location results. In comparison to the standard seismic tomography method, the double-difference tomography method results in a sharper-featured velocity structure that is consistent with the geologic setting. At the same time, it produces absolute and relative event locations accurately, similar to the results obtained by the DD location method developed by Waldhauser and Ellsworth (2000). Our next steps are to apply this algorithm to another test dataset, from Parkfield, California, and then to develop the regional-scale version and apply it to our regional California ground-truth dataset.

OBJECTIVES

The standard processing approach for the determination of seismic event hypocentral locations involves a single-event procedure. Phase arrivals are timed and associated to define an event, and the associated phases are used (potentially along with arrival azimuths and slownesses) to compute a best-fitting location. It has been shown that order-of-magnitude reductions in event location errors and uncertainties are possible if multiple-event techniques are utilized. Recent studies of earthquakes in Hawaii (Rubin et al., 1998), California (Waldhauser et al., 1999), and at the Soultz geothermal area (Rowe et al., 2002), and of explosions at the Balapan test site (Phillips et al., 2001; Thurber et al., 2001), and others, have demonstrated in a dramatic fashion the substantial improvement in the definition of seismogenic features or in the accuracy of relative locations of ground-truth events that is possible with multiple-event methods utilizing high-precision arrival-time estimation.

Our research program consists of four components, each involving some aspect of multiple-event analysis: (1) high-precision WCC for relative arrival time estimation; (2) robust event clustering; (3) waveform decomposition and source wavelet deconvolution reshaping; (4) double-difference (DD) multiple-event location and tomography. In this paper, we will focus on our accomplishments under components 1, 2, and 4, plus our work on ground-truth datasets used for testing our analysis methods.

RESEARCH ACCOMPLISHED

Ground-Truth Datasets

We are constructing two regional ground-truth datasets, one for New Mexico and one for California. The former dataset is from the New Mexico Tech short-period network and is dominated by small explosions, whereas the latter is from the UC-Berkeley broadband network and contains relatively large earthquakes. The New Mexico dataset consists of two parts, one spanning July 1997-February 1998 that has undergone a complete repicking, relocation, WCC, and clustering analysis, and the other spanning January 2001-present that is being prepared for real-time testing. The California dataset was extracted from the Northern California Earthquake Data Center (NCEDC). We first affirmed the quality of the NCEDC catalog location information by carrying out a DD location analysis using catalog time-difference data for 130 events and 23 stations. We found that the DD locations reproduced those in the catalog within 2 to 3 km (in epicenter and depth) on average. We then used a combination of automatic and manual picking to augment and improve the available P arrival picks, and to provide analyst pick weights.

Waveform Cross-Correlation

WCC can be a powerful tool for improving earthquake phase identification and subsequent hypocenter locations. Our software is being built upon an initial package that was designed to retroactively process large catalogues having existing phase picks (P and S). This package compares similar waveforms and identifies families of events meeting specified cross-correlation thresholds, based on a master station or suite of stations. Within families of similar earthquakes, waveforms are compared on a station-by-station basis and their picks are adjusted by applying an L1-norm based conjugate gradient technique to the matrix of first differences. Consistent, mean-adjusted picks are re-entered into trace headers for other uses such as waveform stacking, hypocenter location or seismic tomography.

The WCC program has some features, which help it to perform in an auto-adaptive manner. These include: adaptive, full-spectrum cross-coherency-based prefiltering; a multi-component signal covariance estimator that provides automatic, adaptive polarization filtering to optimize signal linearity; and the use of multiple eigentapers in the subsample cross-spectral correlation step to reduce signal leakage and variance when estimating the signal cross-spectra. We have adapted the cross-correlation program with the addition of eigentapers in the coarse (integer-sample) cross-correlation step, and we are in the process of comparing this approach to coarse lag estimation with the previous method of applying multiple narrow-band filtering. Both approaches provide a means of estimating linearly independent realizations of the time series and therefore permitting quantitative error estimates for the integer correlation step; in future work we will combine the two strategies via application of multiple eigenwavelet methods.

The correlator has also been adapted so that its output may optionally be generated in a format that is compatible with the hypoDD program, so that joint location may be performed using the cross-correlation comparisons without actually solving for consistent pick lags and correcting the picks themselves. Further, the correlator now has an option of generating only one set of first-differences, for applications in which it is only desired to compare a set of "reference events" to the trace of a single ("test") event. This option is being tested in our hierarchical approach described in the next section.

Event Clustering

Waveform clustering, used to segregate signals in to families of similar events, has been tested with a variety of approaches. One successful approach has been to identify clusters based on very high standards of cross-correlation (0.8 or 0.85), resulting in many small multiplets of highly similar events. These are then cross-correlated and consistent pick adjustments are determined via a conjugate gradient solver. Waveforms are aligned on their new picks and stacked to provide a composite waveform representation for the cluster. These stacks are then cross-correlated among the multiplets and inconsistencies in the mean adjusted picks can be corrected by finding consistent adjustments among the stacks. The resulting stack pick lags are propagated to the parent traces. This has been shown to reduce the inter-cluster inconsistencies that result in cluster centroid biases when earthquakes are located using the new picks (these biases existed in the initial catalogue as well). Another related approach that has shown good success is application of the clustering program to the waveform stacks. Those traces whose stacks cluster together based on a high similarity coefficient are joined into larger, second order families. Their member traces are cross-correlated and adjusted for consistency within this larger group. The second-order clusters, following pick adjustment, are stacked yet again and their stacks are compared for similarity. This process may be performed in a hierarchical manner until stacks fail to cluster. Final adjustment of mean centroid picks on the ultimate stacks has been tested using an autopicker; this works well when many traces contribute to the stack but we are still testing different methods of estimating pick uncertainty from the autopicker functions. Phase-weighted stacking, jackknifing methods or multiple-frequency-band approaches may provide the best uncertainty estimates.

Most seismic stations exhibit signal quality problems to some extent or another. When analyzing datasets that cover a wide geographic expanse and a wide magnitude range, any master station may at times have poorer signal quality than other sensors in a network, either because of clipping for a large, nearby event, or poor signal/noise for smaller, more distant ones. Reliance on a single station to perform all similarity choices is therefore not generally the best approach, and we are testing the success of a more adaptive technique where two or more stations may have their waveform similarity matrices compared for consistency, particularly among events that have been orphaned in the clustering step for one of the stations.

Often the first arrival is very emergent and only later portions of the signal can be compared. In these cases, it is useful to have a sliding correlation window to search for similarity later in the event coda. We have modified the correlator to permit this, and have performed interactive testing to demonstrate that sometimes highly similar events, whose first arrivals were uncorrelatable, can be well aligned using the secondary phases. One does not generally expect even among similar events that alignment of later phases will necessarily optimally align the first arrivals; however, among events whose similarity has been established at several correlation lengths for several stations, this provides a means of identifying arrivals at noisier stations and improving the ability to estimate hypocenters for these events. We see this approach as a potential tool in generating autopicks at stations with poorer S/N; if a new event has been identified as belonging to a family of highly similar events, the pick for the poor station may be predicted based on its picks for better-recorded events in the same family, then the validity of the autopick may be verified (and its time adjusted) through comparing later, stronger portions of the waveforms.

WCC analysis of P wave data has shown the ability to identify event clusters based on the cross-correlation information. In a small study region, P wave data might suffice for identifying clusters and hence the source position. However, the smaller window lengths and high-frequency data used in WCC P-wave analysis limits the ability to construct unique location information in a larger study region. Shearer (1994) has demonstrated the use of low-frequency data (3 mHz to 0 0.1 Hz) for global event location and Withers et al. (1999) have successfully applied a similar method to local and regional data utilizing coarse and fine spatial grids. A hierarchical clustering analysis incorporating both the statistical advantages of cluster analysis with adaptive use of grid size and frequency content of the data set offers an alternate means to locate earthquakes. The order of magnitude reductions in location errors found with the use of WCC analysis for event clusters suggest a similar improvement can result from our

hierarchical clustering analysis, with location accuracy limited mainly by the distribution of the ground truth (reference event) locations, binning interval, and the clustering statistics.

We present the initial results on hierarchical WCC/clustering analysis on the California GT dataset, based on WCC analysis of P through surface waves in a first step and the P phase in a second step. We binned the events in 0.1° latitude and longitude bins and in 2.5 km depth bins. The largest magnitude events per bin comprise our 162 reference events, and the next largest 24 events are used for the test dataset. The reference events are displayed in Figure 1a, and the test events and stations used for the preliminary hierarchical analysis are shown in Figure 1b. The WCC analyses for the two steps were accomplished in a similar manner. Waveform data from each test event were cross-correlated against the reference event waveforms to determine the maximum value, in the whole region using low-frequency data in step one, and in a 2° region about the step-one location estimate using high-frequency data in step two. The maximum cross-correlation value per bin from the 7 stations was contoured as an indicator of test event location. Figures 2a and b display the results for a test event located near Los Angeles. For this example, the WCC analysis is performed on the vertical component data for both steps. The estimated location for this event falls with 25 km of the catalog location using the low-frequency data, and improves to 7.5 km using high-frequency data. The next step is to use WCC on the test event and nearby reference events followed by DD location of the event group.

Double-Difference Location and Tomography

The accuracy of event hypocenters is determined by several factors, including the network geometry, available phases, and arrival time accuracies (Pavlis, 1986). If more phases are available, the event hypocenters may be more stable. For example, S-wave phases will be very useful in constraining event depths and providing information that helps to decouple the hypocenters from the structure in the inversion (Gomberg et al., 1990). Due to the presence of noise, the arrival times picked either manually or automatically generally have errors. Recent studies have shown spectacular improvements in location precision for earthquakes and explosions when WCC and event clustering techniques are used to improve arrival time estimates or determine high-precision relative arrival times (VanDecar and Crosson, 1990). Such studies are based on the assumption that waves generated by two similar sources, propagating along similar paths, will generate similar waveforms, and WCC can then be used to determine precise relative arrival times. These studies have demonstrated substantial improvement in the definition of seismogenic features and in the accuracy of relative locations of ground-truth events that is possible using multiple-event methods with high-precision absolute or relative arrival-time data.

We can make an important distinction between the two fundamentally different ways WCC data has been used: (1) by directly using relative arrival times to determine relative event locations (e.g., Got et al., 1994; Waldhauser and Ellsworth, 2000), and (2) by adjusting absolute arrival time picks to minimize discrepancies among relative arrival times (Dodge et al., 1995; Rowe et al., 2002). The advantage of the former approach is that it incorporates all the available information contained within the multitude of relative arrival time differences with a direct measure of quality (the correlation value) associated explicitly with each datum. A disadvantage is that some simplifying assumption needs to be made to derive the locations from the arrival time differences. For example, in the method of Got et al. (1994), the events in a cluster have precisely the same take-off angle and azimuth to each station. As a result, the derived locations are ultimately relative, not absolute, so that some assumption must be made to end up with useful event coordinates (e.g., final locations are computed relative to a catalog-based cluster centroid). Waldhauser and Ellsworth (2000) proposed a different location algorithm, in which the spatial partial derivatives for the set of events are evaluated at different reference points. Thus the absolute event locations are obtained, rather than the relative locations. It is assumed, however, that the path anomalies from velocity heterogeneity are location independent. This assumption is valid for closely spaced events, but is not true for far apart events. As a result, the event locations are biased due to velocity heterogeneity (Wolfe, 2002). In contrast, the latter approach uses the relative arrival times to determine a much smaller number of adjusted arrival time picks, but these picks are absolute arrival times and so can be used to determine absolute locations (in an existing velocity model).

We have developed a new algorithm that combines the advantages and avoid the disadvantages of the above approaches. It is based on the code hypoDD of Waldhauser and Ellsworth (2001), and makes use of both absolute and relative arrival time data. The method determines a three-dimensional (3D) velocity model jointly with the absolute and relative event locations. This approach has the advantage of including relative arrival times with their quality values along with absolute arrival times, thereby not discarding valuable information by only using adjusted

picks, and at the same time dispensing with simplifying assumptions about ray path geometries or path anomalies and producing absolute locations, not just relative locations. To demonstrate the effectiveness of the method, we have applied this method to the Hayward fault dataset of Waldhauser and Ellsworth (2002) to show the fine scale structure of seismicity and to study the local three-dimensional seismic velocity structure.

The body wave arrival time T from an earthquake i to a seismic station k is expressed using ray theory as a path integral

$$T_k^i = \tau^i + \int_i^k u\,ds \tag{1}$$

where τ is the origin time of event i, u is the slowness field and ds is an element of path length. The source coordinates (x_1, x_2, x_3), origin times, ray-paths, and the slowness field are unknown model parameters. The relationship between the arrival time and the event location is nonlinear, so a truncated Taylor series expansion is generally used to linearize Equation (1). The misfit between the observed and the predicted arrival times can be linearly related to the perturbations to the hypocenter and velocity structure parameters

$$r_k^i = \sum_{l=1}^{3} \frac{\partial T_k^i}{\partial x_l^i} \Delta x_l^i + \Delta\tau^i + \int_i^k \Delta u\,ds \tag{2}$$

If we subtract from Equation (2) an equivalent equation for event j, we have

$$r_k^i - r_k^j = \sum_{l=1}^{3} \frac{\partial T_k^i}{\partial x_l^i} \Delta x_l^i + \Delta\tau^i + \int_i^k \Delta u\,ds - \sum_{l=1}^{3} \frac{\partial T_k^j}{\partial x_l^j} \Delta x_l^j - \Delta\tau^j - \int_j^k \Delta u\,ds \tag{3}$$

Assuming that these two events are near each other so that the paths from these two events to the common station are almost identical and the velocity structure is known, then Equation (3) can be simplified as

$$r_k^i - r_k^j = \sum_{l=1}^{3} \frac{\partial T_k^i}{\partial x_l^i} \Delta x_l^i + \Delta\tau^i - \sum_{l=1}^{3} \frac{\partial T_k^j}{\partial x_l^j} \Delta x_l^j - \Delta\tau^j \tag{4}$$

Use of Equation (4) is known as the "double-difference" (DD) earthquake location algorithm (Waldhauser and Ellsworth, 2000). Wolfe (2002) has carried out an elegant comparison of this method to those of Jordan and Sverdrup (1981) and Got et al. (1994), pointing out the general similarities and subtle differences, and discussing the advantages and limitations of each method. Her most important conclusion is "that when the path anomalies from velocity heterogeneity change strongly with earthquake position, the bias effects can be reduced in the relative locations between closely spaced earthquakes, but the effects cannot be reduced in the relative locations between earthquakes spaced far apart." Two assumptions in the Waldhauser and Ellsworth (2000) method are key: an *a priori* layered velocity model is assumed, and they add a constraint equation forcing the mean shift of all earthquakes to be (approximately) zero.

We can generalize the 3D DD location method to jointly determine the 3D velocity structure and the (absolute) event locations. The equations for the DD tomography algorithm, hypo3VDD, are:

$$\begin{aligned} r_k^i - r_k^j &= \sum_{l=1}^{3} \frac{\partial T_k^i}{\partial x_l^i} \Delta x_l^i + \Delta\tau^i + \int_i^k \Delta u\,ds - \sum_{l=1}^{3} \frac{\partial T_k^j}{\partial x_l^j} \Delta x_l^j - \Delta\tau^j - \int_j^k \Delta u\,ds \\ r_k^i &= \sum_{l=1}^{3} \frac{\partial T_k^i}{\partial x_l^i} \Delta x_l^i + \Delta\tau^i + \int_i^k \Delta u\,ds \end{aligned} \tag{5}$$

Our tomography algorithm incorporates first-difference smoothing constraints, with a greater smoothing constraint weight applied to horizontal direction than the vertical (since vertical velocity changes are generally expected to be greater).

Figure 3a shows the location results from the application of hypo3VDD to the Hayward dataset. The earthquake locations are quite consistent with those from hypoDD (Figure 3b), but with a systematic SW shift. For comparison, we also relocate the events by using the standard tomography method with only the absolute catalog data (Figure 3c). We see that the event locations are still scattered, comparable to the catalog locations (Figure 3d). The velocity model shows a clear contrast across the fault, with the SW side faster, as expected. Figure 4a shows across-strike vertical sections through the velocity model resulting from the DD tomography method. We see that the Hayward fault is marked by a strong velocity contrast, similar to the results shown in Hole et al. (2000). This contrast persists vertically beneath the surface trace of the fault to the maximum depths constrained by the model. Higher velocity rocks are located to the west, consistent with the local geological setting. The strong velocity contrast near the surface is due to the boundary between the Franciscan terrane and the Great Valley Sequence. Figure 4b shows across-strike vertical sections through the velocity model from the standard tomography method with only absolute catalog data. Comparing Figures 4a and b, we note that the velocity contrast boundary is more consistent with the event locations and the velocity contrast is sharper in the model from the DD tomography method. DD tomography yields event locations that are more linear and concentrated (less "fuzzy") than those from the standard tomography method. Consequently, this makes the velocity contrast sharper and more consistent with the event locations. Our next step is to extend this method to regional scales.

CONCLUSIONS AND RECOMMENDATIONS

We have assembled the initial set of components and tools for our integrated multiple-event analysis process. These components include (1) regional ground truth datasets, (2) an improved and more versatile WCC algorithm, (3) a more sophisticated event clustering scheme, including the use of multiple waveform windows, and stacking and automatic stack pick readjustment, (4) a preliminary hierarchical process for WCC/clustering/location analysis using a set of reference events, and (5) a new DD tomography algorithm. Our recommendations for further work include (1) finalizing the ground truth datasets and submitting them to the knowledge base system, (2) adding a more user-friendly front end to the WCC software, (3) adding more sophisticated processing elements to the hierarchical WCC/clustering/location processing, including the testing of schemes for determining and/or correcting for event depths and creating generalized reference waveforms, (4) adding DD location capability to the MatSeis location software and/or LocSAT, and (5) creating a regional-scale version of our new DD tomography algorithm.

REFERENCES

Dodge D. A., G. C. Beroza, and W.L. Ellsworth (1995), Foreshock sequence of the 1992 Landers, California, earthquake and its implications for earthquake nucleation, *J. Geophys. Res.,* 100, 9865-9880.

Gomberg, J. S., K. M. Shedlock, and S. W. Roecker (1990), The effect of S-wave arrival times on the accuracy of hypocenter estimation, Bull. *Seism. Soc. Am.*, 80, 1605-1628.

Got, J.-L., J. Frechet, and F. W. Klein (1994), Deep fault plane geometry inferred from multiplet relative relocation beneath the south flank of Kilauea, *J. Geophy. Res.,* 99**,** 15,375-15,386.

Hole, J. A., T.M. Brocher, S. L. Klemperer, T. Parsons, H. M. Benz, and K.P. Furlong (2000), Three-dimensional seismic velocity structure of the San Francisco Bay area, *J. Geophys. Res.,* 105**,** 13,859-13,874.

Jordan, T. H. and K. A. Sverdrup, (1981) Teleseismic location techniques and their application to earthquake clusters in the south-central pacific, *Bull. Seism. Soc. Am.*, 71, 1105-1130.

Pavlis, G. L. (1986), Appraising earthquake hypocenter location errors: a complete practical approach for single-event locations, *Bull. Seism. Soc. Am.,* 76**,** 1699-1717.

Phillips, W.S., Hartse, H. E., and Steck, L. K. (2001), Precise relative location of 25 ton chemical explosions at Balapan using IMS stations, *Pure Appl. Geophys.*, 158, 173-192.

Rowe, C. A., R. C. Aster, W. S. Phillips, R. H. Jones, B. Borchers, and M. C. Fehler (2002), Using automated, high-precision repicking to improve delineation of microseismic structures at the Soultz geothermal reservoir, *Pure Appl. Geophys.*, 159, 563-596.

Rubin, A., D. Gillard, and J.-L. Got (1998), A re-examination of seismicity associated with the January 1983 dike intrusion at Kilauea volcano, Hawaii, *J. Geophys, Res*. 103, 10,003-10,015.

Shearer, P.M. (1994), Global seismic event detection using a matched filter on long-period seismograms, *J. Geophys. Res*., 99, 13,713-13,725.

Thurber, C., C. Trabant, F. Haslinger, and R. Hartog (2001), Nuclear explosion locations at the Balapan, Kazakhstan, nuclear test site: the effects of high-precision arrival times and three-dimensional structure, *Phys. Earth Planet. Int.*, 123, 283-301.

VanDecar, J.C. and R. S. Crosson (1990), Determination of teleseismic relative phase arrival times using multi-channel cross-correlation and least squares, *Bull. Seism. Soc. Am.*, 80, 1548-1560.

Waldhauser, F., and W. L. Ellsworth, A double-difference earthquake location algorithm: Method and application to the Northern Hayward Fault, California, *Bull. Seism. Soc. Am.,* 90, 1353-1368, 2000.

Waldhauser, F., and W. L. Ellsworth, Fault structure and mechanics of the Hayward Fault, California, from double-difference earthquake locations, *J. Geophys. Res.,* 107, ESE 3, 1-13, 2002.

Waldhauser, F., W.L. Ellsworth, and A. Cole (1999), Slip-parallel seismic lineations on the northern Hayward Fault, California, *Geophys. Res. Lett*., 26, 3525-3528.

Withers, M., R. Aster, and C. Young (1999), An automated local and regional seismic event detection and location system using waveform correlation, *Bull. Seism. Soc. Am.*, 89, 657-669.

Wolfe, C. J. (2002), On the mathematics of using difference operators to relocate earthquakes, *Bull. Seism. Soc. Am*., in press.

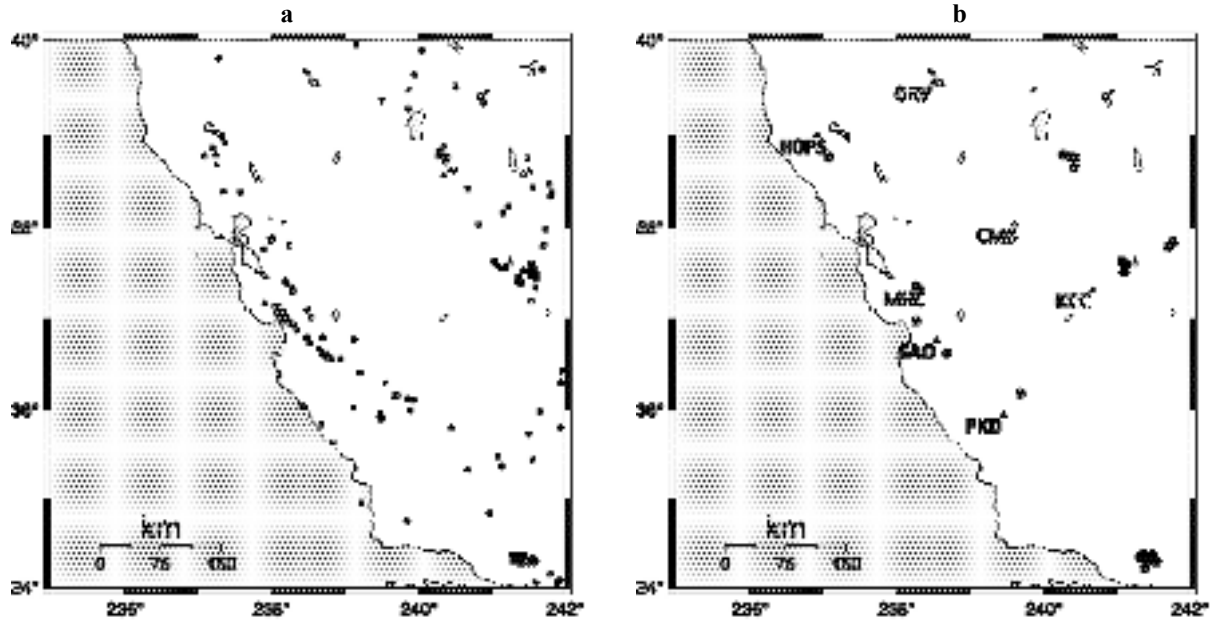

Figure 1. Maps of (a) reference events and (b) test events and test stations from our California ground-truth dataset.

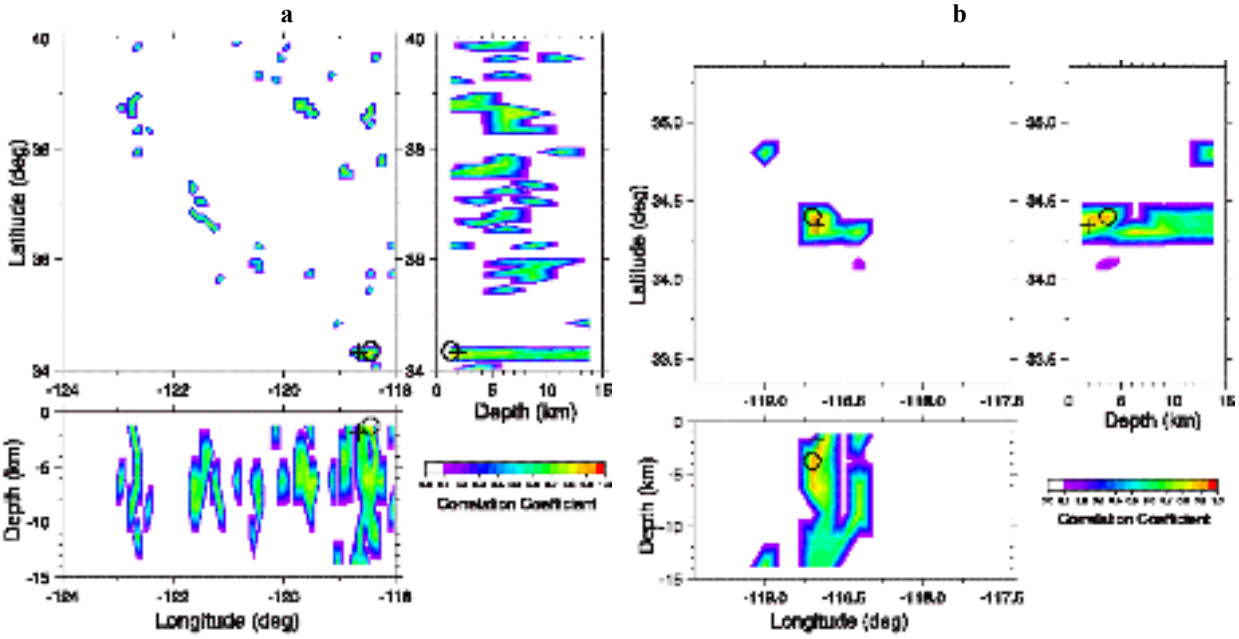

Figure 2. Contour plots (map view and depth sections) of the maximum cross-correlation value per bin for the 7 stations for a test event (located at lat. 34.3°, lon. -118.58°, and depth 1.8 km, cross) correlated against the set of reference events in the (a) low-frequency band (step one) and (b) high-frequency band (step two). Note the good low-resolution location estimate on the left (circle) and the improved high-resolution location estimate (circle) on the right.

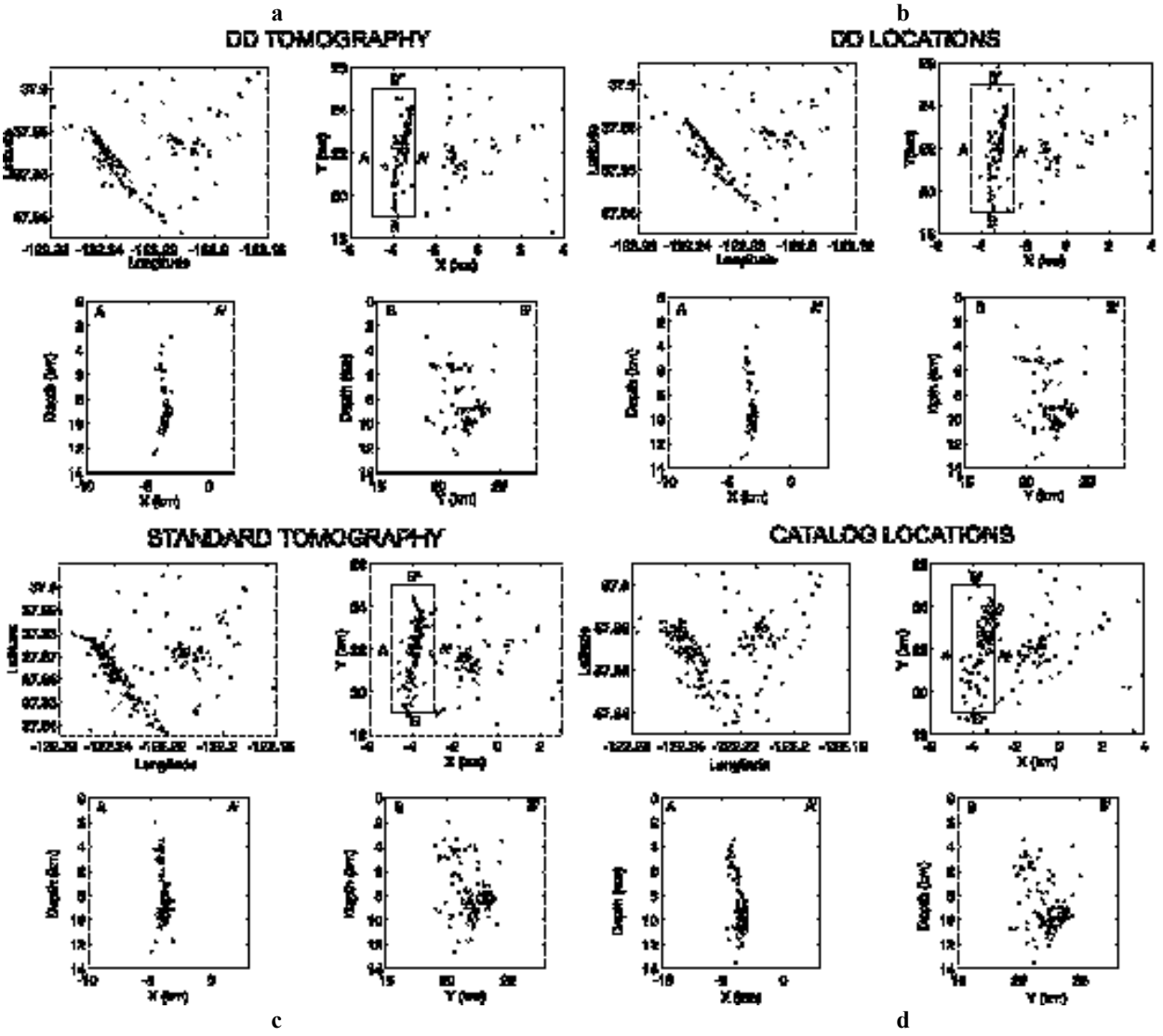

Figure 3. Comparison of earthquake locations along the Hayward fault determined using (a) DD tomography, (b) DD location, (c) standard tomography, and (d) catalog data (no DD data). Each part shows a lat-lon plot (upper left) and zoomed-in plots (rotated to fault-parallel/fault-normal) of epicenters (upper right) and fault-normal (lower left) and fault-parallel (lower right) depth sections. Note how closely the hypocenters in panels a and b resemble each other, but with a systematic SW shift. The tight clustering is not evident in either the standard tomography solution (c) or the catalog locations using absolute picks only (d).

a **b**

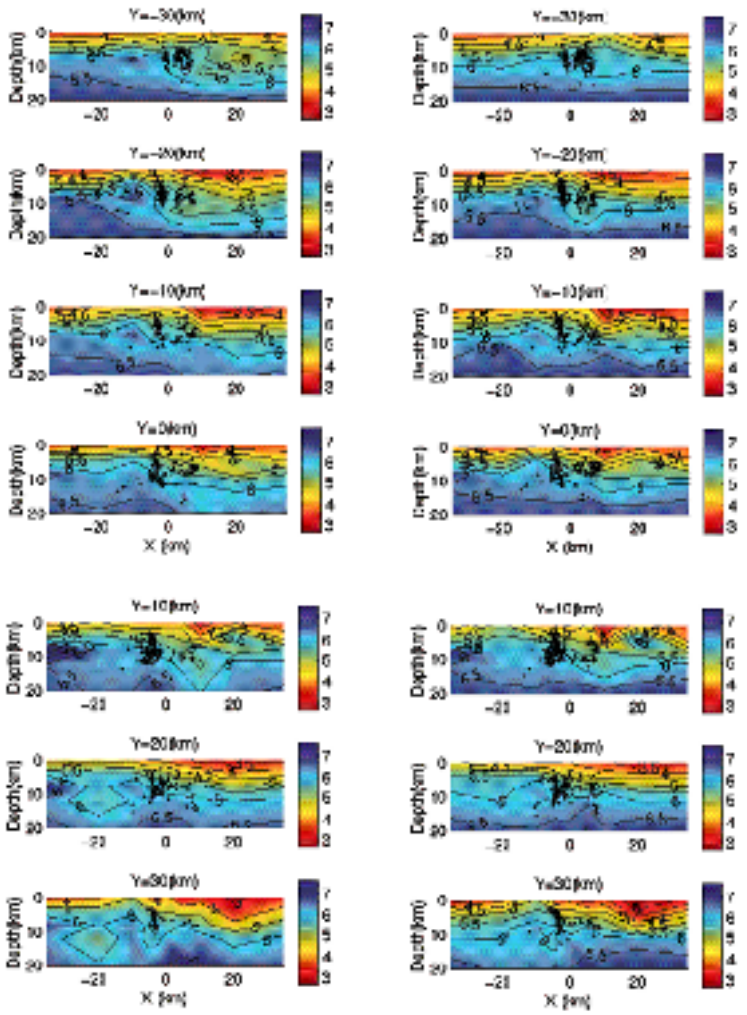

Figure 4. (a) The left-hand panels show fault-normal slices through the DD tomography model. The model has sharper features and a better correspondence between the main region of seismicity and the position of the sharp velocity contrast compared to the standard results (Figure 4b). (b) The right-hand panels show fault-normal slices through the standard tomography model. The model has features that are less sharp and a poorer correspondence between the main region of seismicity and the position of the velocity contrast than the DD results